RI 9554

RI | 9554

REPORT OF INVESTIGATIONS/1995

Petrographic and Geochemical Analyses of Leach Samples From Artillery Peak, Mohave County, AZ

UNITED STATES DEPARTMENT OF THE INTERIOR

UNITED STATES BUREAU OF MINES

U.S. Department of the Interior
Mission Statement

As the Nation's principal conservation agency, the Department of the Interior has responsibility for most of our nationally-owned public lands and natural resources. This includes fostering sound use of our land and water resources; protecting our fish, wildlife, and biological diversity; preserving the environmental and cultural values of our national parks and historical places; and providing for the enjoyment of life through outdoor recreation. The Department assesses our energy and mineral resources and works to ensure that their development is in the best interests of all our people by encouraging stewardship and citizen participation in their care. The Department also has a major responsibility for American Indian reservation communities and for people who live in island territories under U.S. administration.

Report of Investigations 9554

Petrographic and Geochemical Analyses of Leach Samples From Artillery Peak, Mohave County, AZ

By Susan E. Brink, Rolland Blake, and Dianne Marozas

UNITED STATES DEPARTMENT OF THE INTERIOR
Bruce Babbitt, Secretary

BUREAU OF MINES
Rhea Lydia Graham, Director

International Standard Serial Number
ISSN 1066-5552

CONTENTS

ILLUSTRATIONS

TABLES

TABLES—Continued

UNIT OF MEASURE ABBREVIATIONS USED IN THIS REPORT

Metric Units

cm	centimeter	mL	milliliter
cps	count per second	mL/min	milliliter per minute
deg	degree	mm	millimeter
g	gram	Mt	million metric tons
g/L	gram per liter	nA	nanoampere
kg	kilogram	t	metric ton
km	kilometer	vol %	volume percent
km^2	square kilometer	wt %	weight percent
kPa	kilopascal	μm	micrometer
kV	kilovolt	°C	degree Celsius
m	meter		

U.S. Customary Units

psi	pound (force) per square inch

PETROGRAPHIC AND GEOCHEMICAL ANALYSES OF LEACH SAMPLES FROM ARTILLERY PEAK, MOHAVE COUNTY, AZ

By Susan E. Brink,[1] Rolland Blake,[1] and Dianne Marozas[2]

ABSTRACT

The first step in determining whether Mn can be recovered by in situ leaching is to develop and test a selective lixiviant. Two column leach tests and one core leach test were conducted by the U.S. Bureau of Mines on Mn oxide ore using aqueous sulfur dioxide (SO_2) as the lixiviant. The column tests showed that aqueous SO_2 could selectively dissolve available Mn oxides from calcite-rich ore in a heap leach system. However, the core test showed that calcite gangue side reactions can have pronounced negative effects on the likelihood of successful in situ leaching of a calcite-rich ore with aqueous SO_2. Petrographic and geochemical analyses showed that both Mn (IV, III) oxides and calcite were dissolved. The abundance of dissolved Ca caused precipitation of gypsum. Acid consumption by calcite dissolution caused a rise in pH that caused the SO_2/S species to shift to SO_3^{2-} (sulfite), which hindered reductive dissolution of Mn oxide. Gypsum precipitation did not affect complete leaching of the rock fragments in the column tests; however, it plugged the natural permeability in the core. Manganese recoveries were high for the column tests and low for the core test.

[1]Geologist, Twin Cities Research Center, U.S. Bureau of Mines, Minneapolis, MN.
[2]Geochemist, Sandia National Laboratory, Albuquerque, NM.

INTRODUCTION

The U.S. Bureau of Mines (USBM) is conducting research to develop cost-effective, environmentally compatible, advanced technologies for the selective extraction of critical and strategic metals, such as Mn, Co, and Cr from ores of these metals. In situ leach mining requires less capitol investment, labor force, and energy consumption than conventional mining and milling, while offering better health and safety conditions for mine workers and causing less environmental impact. Through column leach tests, the USBM has determined that some types of Mn oxide ore have the potential for recovery by in situ leach mining techniques (Khalafalla and Pahlman, 1981; Marozas and others, 1992). In this study, column leaching tests were conducted on calcite ($CaCO_3$) rich Mn oxide ore to determine the selectivity of the aqueous SO_2 lixiviant for Mn over Fe and Ca. A core leaching test was also conducted to more closely simulate the natural permeability of a calcite-rich Mn oxide ore in an in situ leach mining system.

LOCATION AND GENERAL GEOLOGY OF DEPOSIT

The Artillery Peak Mn district is located in southern Mohave County, AZ, approximately 64 km (40 miles) northwest of Phoenix, AZ. Syngenetic Mn oxide was deposited with early Pliocene alluvial fan and playa sediments, the Chapin Wash Formation, in a large fault basin between the Artillery and Rawhide Mountains. The Chapin Wash Formation covers an area of approximately 65 km^2 (25 square miles) and consists of arkosic sandstones, siltstones, conglomerates, mudstones, and tuffs. Estimated reserves for the Artillery Peak District are 158.8 Mt of material containing 5.5% to 6.3% MnO_2 (manganese dioxide) and 4.3% Fe_2O_3 (hematite) (Kumke and others, 1957). The north and south Maggie blocks of the Maggie Canyon area consist of higher grade material. The north Maggie block contains 13.6 Mt of material that averages 10.3% MnO_2 and the south Maggie block consists of a 6.1-m thick manganiferous layer that contains 1.8 Mt of material grading 15.8% MnO_2.

The location of samples selected for column and core leach tests in this study are as follows: The level-1 ore sample used in one of the column leach tests is from the toe of Cobweb Hill on the Lake property within the Artillery Peak District. It contained 4.9% MnO_2. The GP-1 ore sample used in the second column leach test was taken from a high-grade dump on the Lake property. It contained 42.7% MnO_2. A 10-cm-diameter interval of core, labeled "massive 2," was taken below the tuff layer on Cobweb Hill, and this sample was used for the core leach test. Sample massive 2 contained 21.0% MnO_2.

SELECTIVE LEACHING OF ARTILLERY PEAK ORE

Selective recovery of Mn by in situ leaching from most Mn oxide mineral deposits will require a lixiviant that is chemically selective because of the intimate textural relationship between Fe oxide and Mn oxide minerals. Sulfur dioxide (SO_2) has been extensively investigated for selective Mn leaching because it is capable of rapidly dissolving acid-resistant Mn oxides while only slowly leaching many Fe gangue minerals. Khalafalla and Pahlman (1981) reported results that demonstrate the use of SO_2 for selective extraction of critical and strategic metals (i.e., Mn, Co, and Ni) from Pacific ferromanganese nodules. They reported that increasing the ratio of SO_2 in the lixiviant to the mass of nodules leached results in a reproducible sequence of different metals being preferentially leached. Manganese was leached first, followed by nickel, cobalt, iron, aluminum, and copper.

Pahlman and Khalafalla (1988) reported experimental data on SO_2 leaching of Mn ores that are relevant to in situ leach mining. They presented results from batch and column leaching of 25 samples from U.S. Mn deposits exposed to 5 to 6.4 vol % SO_2 solutions. They achieved typically >90% Mn recoveries for Mn oxides and <10% Fe recovery when Fe_2O_3 is the most abundant Fe-bearing gangue mineral. When Fe carbonate (siderite) and hydroxide (goethite) are present, selectivity is reduced because Fe in these minerals is readily dissolved by the acidic SO_2 solution. Pahlman and Khalafalla did not look at textural considerations, which also may have had an effect on the dissolution rates of Mn, Fe, and Ca minerals.

COLUMN LEACH TESTS

PRELEACH GEOLOGIC CHARACTERIZATION

Two column leach tests were conducted on rock samples collected from the Artillery Peak deposit. Preleach petrographic observations of thin sections and X-ray diffraction (XRD) analysis of whole-rock powders of these two ores (level-1 and GP-1) were performed by Saini-Eidukat and Adamson (USBM progress report, 1990). A

summary of their findings follows. The arkosic sandstone is fine to medium grained and ranges from grain supported to matrix supported. The matrix is calcite and Mn oxide cement. The felsic grains are angular to subrounded and consist of quartz, microcline, and plagioclase. Most of the feldspar grains show variable sericitization and calcite has replaced some grains. XRD identified cryptomelane (KMn_8O_{16}) and hollandite ($BaMn_8O_{16}$) as specific Mn minerals. However, representative electron microprobe wavelength dispersive spectrometer (WDS) microanalyses (table 1) of the Mn material in sample level-1 showed that the cryptocrystalline Mn material consists of a mixture of cryptomelane and hollandite, with a few spot analyses of coronadite ($PbMn_8O_{16}$). Figure 1 shows the variation in K and Ba of several WDS microprobe spot analyses of the Mn material. Two spot analyses that contained Pb are also plotted.

Table 1.—Representative WDS microprobe analyses of Mn oxides in sample level-1, weight percent

Oxide	Sample			
	1	2	3	4
BaO	9.96	5.07	9.10	13.74
Fe_2O_3	0.87	ND	0.84	0.26
K_2O	1.64	4.08	1.05	1.13
MnO_2	79.36	84.11	75.09	78.54
Na_2O	0.35	0.34	0.23	0.19
PbO	ND	ND	7.54	ND
SiO_2	ND	ND	ND	ND
Total	92.18	93.60	93.85	93.86

ND No data.

Figure 1

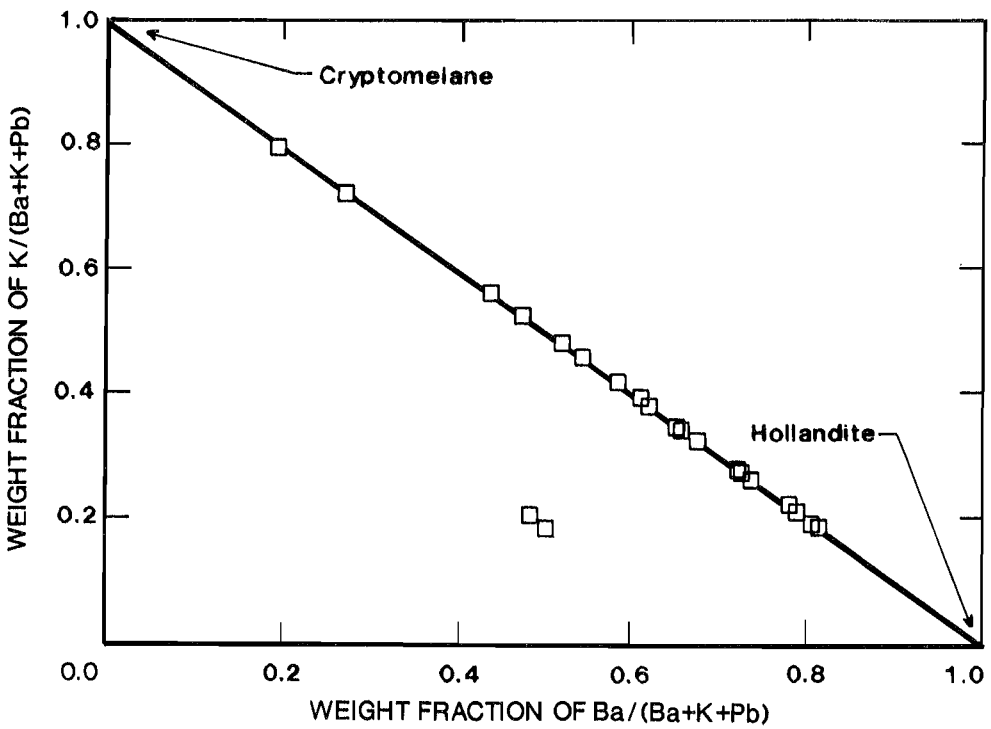

Weight fraction of Ba, K, and Pb filling cation site A of generic hollandite structure $A_{0-2}(MnB)_8O_{16}$ from Artillery Peak sample level-1 analyzed by WDS electron microprobe.

COLUMN LEACH EXPERIMENTS

The column leach tests were conducted in 1-m-long by 10-cm-diameter columns containing 3.5 kg of rock fragments in the minus 2.5-cm to plus 1.3-cm fraction. Solutions of 5 vol % SO_2 were dripped on top of the column at a rate of 1 mL/min. The columns were not tightly sealed and remained at room temperature (24 °C) and unsaturated throughout the experiment. Tests were run until the Mn in the leachate from the column dropped below 1 g/L. Leaching of the GP-1 rock type took approximately 60 days and leaching of the level-1 rock type took approximately 26 days. Leach solution samples were collected at the bottom of the column for chemical analysis for Fe, Mn, Si, Ca, Na, K, and Al by atomic absorption spectrometry or inductively coupled plasma spectrometry.

POSTLEACH GEOLOGIC CHARACTERIZATION

Postleach samples from the column leach tests were analyzed (USBM progress report, 1990) as fragments in Cargille Certified Refractive Index oil with a refractive index number of 1.540. The postleach samples were not made into thin sections because of the friability of the materials. Mn oxides were found as small opaque particles and dark to light brown stains on felsic mineral grains. Traces of hematite (Fe_2O_3) and goethite (FeOOH) were also present. The most significant difference in the preleach and postleach mineralogy occurred in sample level-1, where calcite was found in a preleach sample, but not in a postleach sample, and gypsum ($CaSO_4 \cdot 2H_2O$) was found in a postleach sample, but not in a preleach sample (USBM progress report, 1990).

POSTLEACH GEOCHEMICAL CHARACTERIZATION

Table 2 shows preleach and postleach whole-rock chemical analyses for the column leach tests. Most of the chemical analyses were determined by inductively coupled plasma spectrometry, except for Fe^{2+}, which was determined by titrimetric method, silicon dioxide (SiO_2) by gravimetric method, and S and C by combustion method. The first of the postleach columns shows residual enrichment of some elements because of removal of a significant amount of the rock, mostly as Mn. For example, the Si values for GP-1 show an apparent enrichment from 15.8 to 29.1 wt % Si. Before leaching the rock weighed 3,500 g, but after leaching the rock weighed only 1,768 g. In the second postleach column of table 2, the leached rock values were normalized to the amount of rock leached by multiplying the postleach data by the ratio of grams of leached rock to grams of preleach rock. In this way, the normalized postleach data can be compared with the preleach data to arrive at a more accurate sense of how much of each element was leached or enriched.

The preleach and postleach whole-rock chemical data of the column leached ore, shown in table 2, confirm that Mn was selectively leached over Fe. Almost all of the Mn was leached, while less than half of the Fe was leached from the rock. It is also apparent that Ba, which occurs in the Mn minerals (table 1), was retained in the postleach material. Results for recovery of Mn and Fe in the column leach solutions using level-1 and GP-1 ores are displayed in table 3. The initial amount of Mn, Fe, and Ca present in each preleach sample is also given. Included for comparison are column leach test results on another Artillery Peak sample (AZ-5) reported by Pahlman and Khalafalla (1988). Recoveries for the column leach tests were calculated from preleach and postleach whole-rock chemical analyses, while recoveries for the AZ-5 sample were calculated from leach solution chemistry. The data indicate that Mn can be efficiently recovered from the ores tested, by leaching with SO_2 solutions. Results also show that Mn is selectively leached with respect to Fe.

The preleach rock contains calcite, which is acid soluble. With leaching, all of the C was removed, but only some of the Ca in the rock (table 2). More Ca remains in the rock after leaching than that attributable to refractive Ca in feldspars. The postleach material also contains considerable sulfate enrichment. The preleach and postleach whole-rock chemical data in table 2 suggest that some of the Ca, which dissolved from calcite during leaching, precipitated in the postleach material as gypsum. The precipitation of gypsum in the postleach material is supported by the observation of gypsum in postleach products, as previously mentioned. Calcium extraction in the leach solutions from the rock types tested in this study is also reported in table 3. Pahlman and Khalafalla (1988) reported that, at low SO_2 application rates (1 mL/min) in their column experiments on Artillery Peak samples, calcite solubilization was minimized by the formation of an insoluble reaction layer, which suppressed further leaching of calcite. The reaction layer was composed of a Ca/S compound. When Pahlman and Khalafalla increased the solution application rate from 1 to 5 to 9 to 18 mL/min, Ca solubilization increased for the same ore type. They proposed that this reaction layer was eroded by the increased application rate. Calcium extraction in this study with an application rate of 1 mL/min ranged from 28% to 85% and thus appeared to depend on the ore type.

Table 2.—Whole-rock chemical analyses of preleach and postleach column test samples, weight percent

	Level-1			GP-1		
	Preleach	Postleach	Normalized postleach	Preleach	Postleach	Normalized postleach
Elements:						
Al	5.30	5.06	4.70	3.00	5.80	2.93
Ba	0.41	0.42	0.39	2.00	3.80	1.92
C	0.69	<0.10	<0.10	0.44	<0.10	<0.10
Ca	3.10	2.40	2.23	1.30	0.40	0.20
Fe^{2+}	0.00	0.23	0.21	<0.10	<0.10	<0.10
Fe_{tot}	2.90	1.80	1.67	1.10	1.20	0.61
K	3.70	3.17	2.95	4.00	4.30	2.17
Mg	0.46	0.38	0.35	0.22	0.24	0.12
Mn	3.10	0.11	0.10	27.00	0.59	0.30
Na	1.60	1.17	1.09	0.60	1.00	0.51
P	0.00	0.00	0.00	0.02	<0.01	<0.01
S	0.04	2.00	1.86	0.05	3.80	1.92
Si	28.10	30.02	27.91	15.80	29.10	14.70
LOI	7.20	9.60	8.93	8.30	8.30	4.19
Oxide:						
Al_2O_3	10.01	9.56	8.88	5.67	10.96	5.53
BaO	0.46	0.47	0.44	2.23	4.24	2.14
CaO	4.34	3.36	3.12	1.82	0.56	0.28
CO_3	3.45	0.00	0.00	2.20	0.00	0.00
FeO	4.15	2.57	2.39	1.57	1.72	0.87
Fe_2O_3	0.00	0.30	0.27	0.00	0.00	0.00
K_2O	4.46	3.82	3.55	4.82	5.18	2.61
MgO	0.76	0.63	0.58	0.36	0.40	0.20
MnO_2	4.91	0.17	0.16	42.73	0.93	0.47
Na_2O	2.16	1.58	1.47	0.81	1.35	0.69
P_2O_5	0.00	0.00	0.00	0.05	0.00	0.00
SiO_2	60.12	64.23	59.71	33.80	62.26	31.45
SO_4	0.12	5.99	5.57	0.15	11.39	5.75
LOI	7.20	4.19	8.93	8.30	4.19	4.19
Total	102.14	96.87	95.07	104.51	103.18	54.18

LOI Loss on ignition.

Table 3.—Grade and recovery of Mn, Fe, and Ca for column leach experiments

Sample	Mn		Fe		Ca	
	wt %	% recovered	wt %	% recovered	wt %	% recovered
GP-1	27	99	1	6	1	85
Level-1	3	97	3	42	3	28
AZ-5	3	97	3	9	3	31

CALCITE DISSOLUTION

Evaluation of the amount of calcite in the ore and the degree of calcite dissolution during leaching is an important factor in assessing the viability of in situ leaching at the Artillery Peak site because of some potentially negative side effects that acid consumption and excess Ca can have on the efficiency of leaching. The dissolution of calcite consumes acid and reduces the efficiency of SO_2 leaching of Mn (Marozas and others, 1992). The leaching of Mn oxide minerals with SO_2 is a reductive dissolution reaction and an acid-base reaction that requires a pH of <2.5. This is because sulfurous acid behaves as a weak diprotic acid in which the concentration of the species SO_2, HSO_3^{1-} (bisulfite), and SO_3^{2-} vary as a function of pH (Saini-Eidukat and others, 1993). It is the SO_2 form that is the reactive reducing S species in the Mn oxide system. Sulfur is predominantly in the reactive SO_2 form only when the pH is <2.5. The pH increase owing to acid dissolution of calcite results in a shift in the diprotic acid's equilibrium, as SO_2 reacts to form HSO_3^{1-} and SO_3^{2-}.

A second side effect that Ca has on the efficiency of Mn leaching is particularly troublesome for in situ leaching. When Ca is present in sufficient quantities, it reacts

with the S byproducts of Mn leaching with aqueous SO_2 and precipitates as gypsum in pore spaces, thus reducing system permeability.

Extraction curves for Mn, Fe, and Ca from the Artillery Peak column leach tests for level-1 and GP-1 samples are presented in figure 2. The rate of leaching of Mn from the GP-1 (high-grade) sample was nearly half of that from the level-1 (low-grade) sample. The rate of Ca extraction in experiment GP-1 was rather high at first, exceeding the Mn rate for a time, and then as it leveled off, the Mn

Figure 2

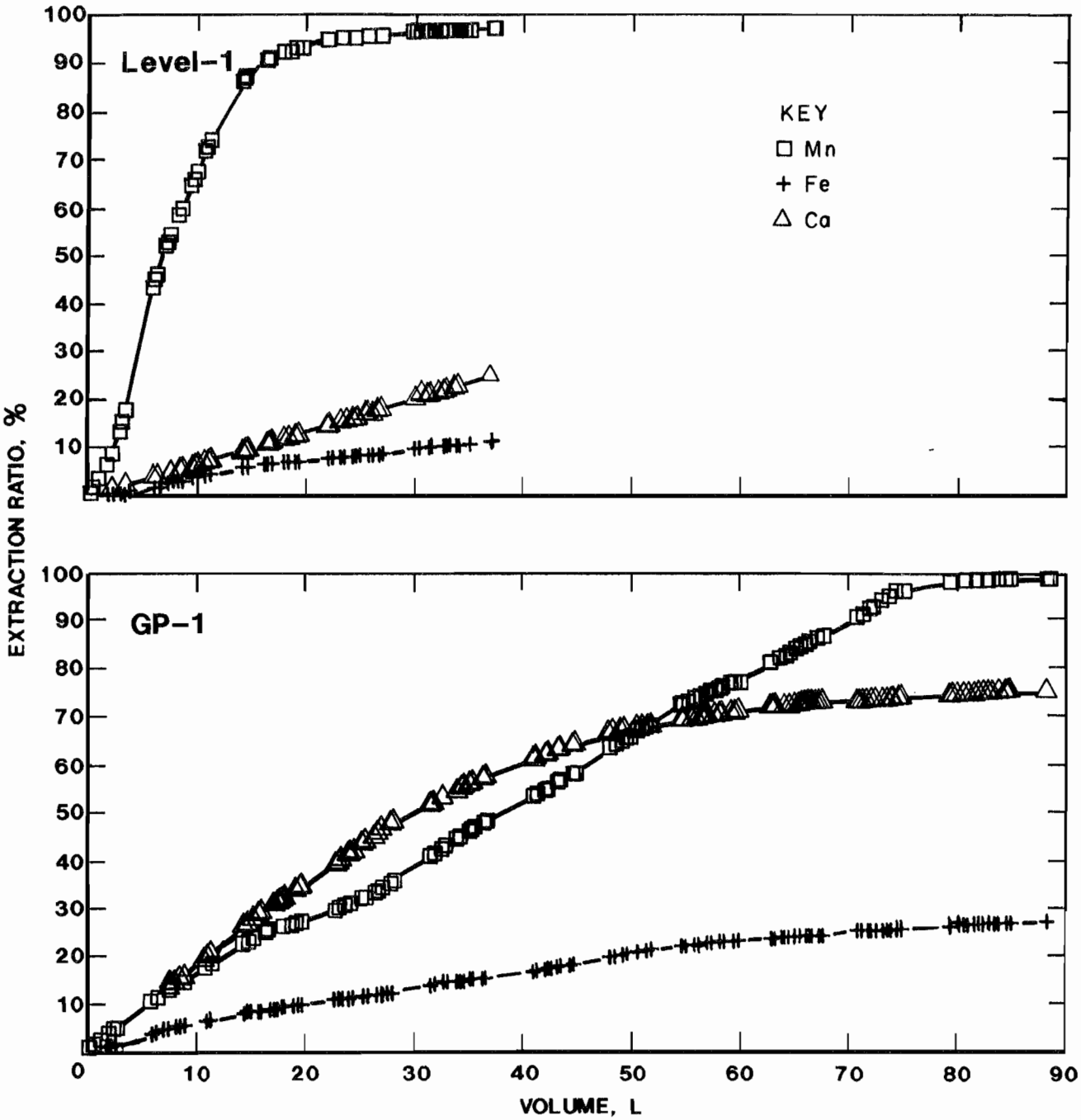

Percentage extraction versus solution volume for column leach tests for level-1 and GP-1 samples.

extraction rate increased. The typical concentrations of Mn, Fe, and Ca in the GP-1 leachate are shown in table 4. During the leach experiment, fresh leach solution was dripped through the column so that a continual supply of acid and aqueous SO_2 was available to the ore. Perhaps, in the GP-1 experiment, as the leach solution contacted calcite, dissolution forced the pH up locally so that the aqueous S shifted from the reductive SO_2 species to the ineffective HSO_3^{1-} and SO_3^{2-} species (Saini-Eidukat and others, 1993). This shift would inhibit the efficient leaching of Mn until the calcite gangue reactivity was reduced by acid dissolution.

Table 4.—Typical leachate concentration of Mn, Fe, and Ca for column and core leach tests, milligrams per liter

Sample	Column (GP-1)	Core (massive 2)
Mn	20,000	13,000
Fe	200	10
Ca	700	3,000

CORE LEACH TEST

Core leach tests add knowledge to that acquired from column leach tests. The experimental conditions in a core leaching test are a step closer to conditions that are expected in the field and yield data not available from column leach tests. In addition to providing chemical data, core leach experiments provide information on permeability changes resulting from mineral dissolution, precipitation, or clay hydration. This is important since the maintenance of adequate permeability is crucial to the success of any in situ leach mining operation. A variety of configurations and materials can be used to conduct core leach tests (Paulson and Kuhlman, 1989), but the basic design is similar in all: A section of core is placed within a piece of pipe, encased in epoxy, and sealed with end caps. Lixiviant is pumped through the core in an axial direction and collected in a closed vessel prior to sampling and analysis (Paulson and Kuhlman, 1989). The differential pressure across the sample is monitored using a pressure transducer to evaluate real-time permeability changes. Upon completion of the experiment, the remaining core material is impregnated with epoxy to preserve delicate structures (Brink and others, 1991) and then prepared for petrographic studies.

PRELEACH GEOLOGIC CHARACTERIZATION

Figure 3 shows the preleach interval of core used in the core leach test. The black rock is an arkosic sandstone that consists of angular to subrounded grains of quartz, microcline, plagioclase, muscovite, and biotite; it is cemented by black Mn oxide minerals, calcite, and an allophane-like, Si/Al-rich phase. Figure 4 is a backscattered electron (BSE) image that shows the preleach texture of the rock. The white rims around the felsic sedimentary grains are Mn oxide. The darker gray material lining interstitial areas between grains is an Si/Al phase and the lighter gray mineral with triangular pits that fills interstitial space is calcite. The quartzofeldspathic grains are medium grained and vary from 10 to 750 μm in diameter, but most range from 200 to 500 μm. Some plagioclase and microcline grains are fresh, while others are slightly to almost completely altered to sericite. The extinction angle of albite twinning was measured on 23 unaltered plagioclase grains and suggests plagioclase compositions ranging from albite (An_0) to andesine (An_{50}). Elongated grains of biotite are greenish brown and essentially unaltered. The Mn oxide that coats the sediment grains is primarily wad (a mixture of amorphous, hydrous Mn oxides) with an outer rim of well crystallized, cryptomelane needles (10 to 20 μm long and 1 to 5 μm wide). These needles protrude into what was interstitial space between grains before further cementation.

The following preleach paragenetic sequence is supported by reflected and transmitted light optical microscopy and BSE images (figure 5) of grain and cement

Figure 3

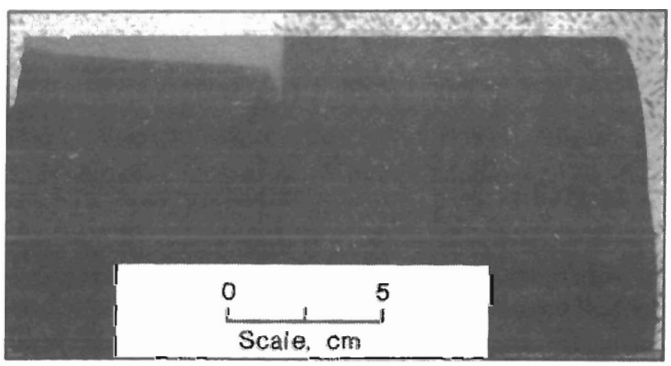

Artillery Peak drill core sample massive 2 before leaching. Rock sample does not show preferred directional fabric such as bedding. Small vugs are lined or filled with calcite, which can be seen as white areas on core.

Figure 4

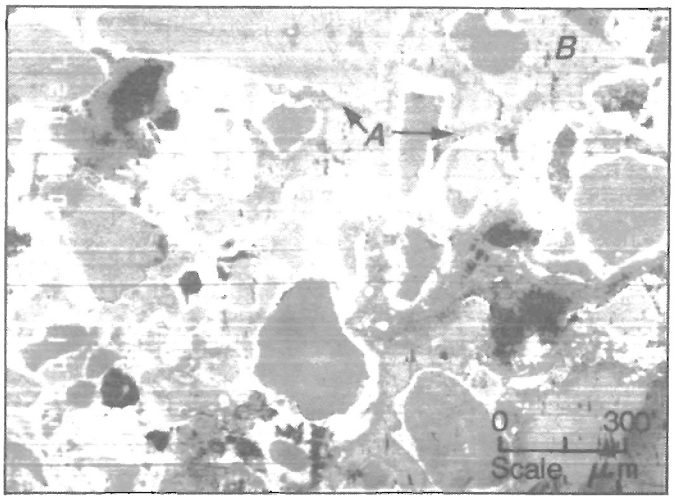

BSE image of preleach ore texture showing subangular grains of arkosic sandstone. Grains are rimmed and cemented by wad (white), allophane-like phase consisting of Si and Al (dark gray) (A), and calcite (light gray) (B).

Figure 5

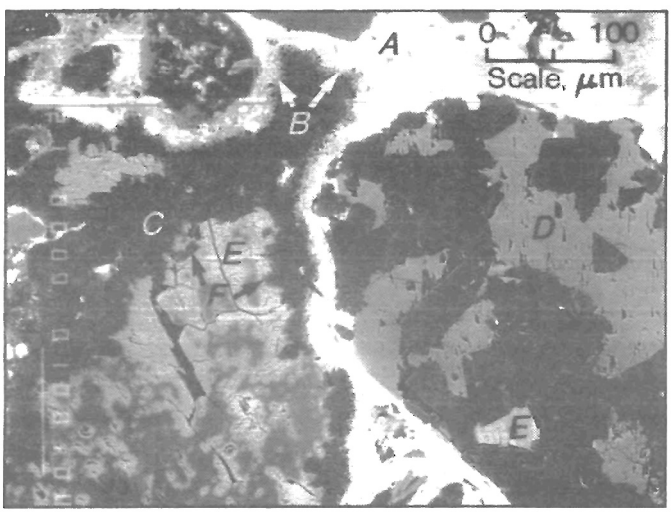

BSE image of preleach ore texture showing paragenetic sequence of mineralization. Interstitial spaces between wad-coated sedimentary grains (A) are rimmed with cryptomelane needles (B), followed by layer of allophane-like material (C) and filled with calcite cement (D). Light material near center of image is gypsum (E) replacing calcite. Altered feldspar grain on right of image contains patches of calcite with triangular pits (D) and lighter patch of gypsum (E). Crystals of allophane-like material are lath shaped (F).

textures. Quartzofeldspathic grains are rimmed with a thin layer of massive wad (figure 5*A*), which cemented the grains in an open framework with abundant pore spaces that are now filled with other minerals. Epigenetic hydrologic processes that formed "hard ore" (Sanford and Stewart, 1948) converted some of the wad to cryptomelane. Cryptomelane occurs as needles (figure 5*B*), which locally rim some of the massive wad and protrude into the interior of the pores. The next layer lining the pore spaces is a thin coating of an allophane-like, Si/Al phase (figure 5*C*). In transmitted light optical microscopy, this material is clear in plane polarized light and black under crossed nicohls. The remaining interstitial space is filled with calcite (figure 5*D*) and rarely with gypsum (figure 5*E*). Notice that crystals of the allophane-like phase have a lath or peg-tooth morphology that protrude into the pore spaces (figure 5*F*). Gypsum, calcite, and the Si/Al material were also observed to have replaced portions of some plagioclase grains (figure 5). Gypsum can be distinguished from calcite in this image by its brightness since gypsum has a higher atomic density than calcite. From the observed textural relationships, it can be seen that gypsum replaced calcite. Gypsum has triangular pits, as are typical for calcite. This example of gypsum occurs naturally in the rock and is not a result of leaching with aqueous SO_2 because the adjacent Mn minerals do not appear to be leached. Well crystallized needles (0.5 to 3 mm long) of gypsum were also observed within vugs in the preleach rock.

CORE LEACH EXPERIMENT

The core leach experiment was performed on a 10-cm-diameter by 20-cm-long drill core sample (labeled "massive 2") of Artillery Peak rock that was drilled from a typical block of rock collected from the deposit. The total weight of the core was 3,145 g. Prior to SO_2 injection, distilled, deionized water was pumped through the core at a rate of 0.05 mL/min to saturate it before leaching. The volume of water pumped into the core at the time of initial fluid breakthrough was 250 mL compared with the volume of the core, 1,383 mL. Thus, 18% of the rock volume was saturated during the preflush. Typical sandstones have porosities in the range of 11% to 16% (Dietrich and others, 1982). Chemical analysis of the water samples showed that Ca and Mg were mobilized by the distilled deionized water flush and that the pH increased from 5.5 to 7.7. After the first sample was collected, the flow rate of the water flush was varied between 1.0 and 0.008 mL/min to establish preleach flow rate conditions for the experiment. After another 250 mL of water was pumped through the core, the injection fluid was switched from distilled water to a 7 wt % solution of aqueous SO_2 at a flow rate of 0.005 mL/min. Solution samples were collected after passing through the core and submitted for chemical analysis for Fe, Mn, Si, Ca, Na, K, and Al by

atomic absorption spectrometry or inductively coupled plasma spectrometry.

During a core leaching experiment, the pump pressure will vary to maintain a constant flow rate through the core. The pump pressure began to increase shortly after the first breakthrough of SO_2 solution through the core. This increase in pressure indicated the beginning of permeability reduction in the core. The pump pressure varied up and down somewhat during the time required for the next several hundred milliliters of solution to pass through the core, but in general, the pump pressure increased. After 800 mL of leach solution was recovered from the core experiment, the pump reached its maximum allowable pressure [6,895 kPa, (1,000 psi)] and the experiment was ended.

POSTLEACH GEOLOGIC CHARACTERIZATION

Cross Section of Leached Core

Figure 6 shows cross-sectional views of the interior of the leached core. The injection end is at the bottom of the photographs. The light horizontal layer is at the injection end and the medium-gray channels of dissolution reach further into the core. In hand samples, these dissolution channels are light orange and more porous and friable than the black, unleached areas. The horizontal band and the vertical channels are a result of leaching and are not primary textures of the massive sandstone.

X-Ray Diffraction

XRD analyses of powdered rock samples were performed using an X-ray powder diffractometer with a Cu-Kα radiation source. Samples were analyzed from the very leached horizontal band at the injection end of the core, the partially leached orange-brown channels of dissolution, and the black, unleached portion of the core (figure 6). X-ray patterns for the unleached (*A*), partially leached (*B*), and very leached (*C*) samples are shown in figure 7. They show a progressive increase in intensity of peaks for gypsum, with a progressive decrease in intensity of peaks for calcite and mica. The XRD pattern for the least leached material identified quartz, calcite, plagioclase, microcline, and mica. The small mica peak represents both biotite and sericite, as determined by light optical microscopy. The major peaks for albite and intermediate anorthite are the same, and the minor peaks overlap with other minerals. Therefore, exact identification of the plagioclase is not available by XRD. No peaks for Mn oxide minerals were present, although the sample was known to contain considerable Mn oxides from chemical analysis, and the XRD pattern had a moderately high background and good peaks for other minerals. Therefore, it is

Figure 6

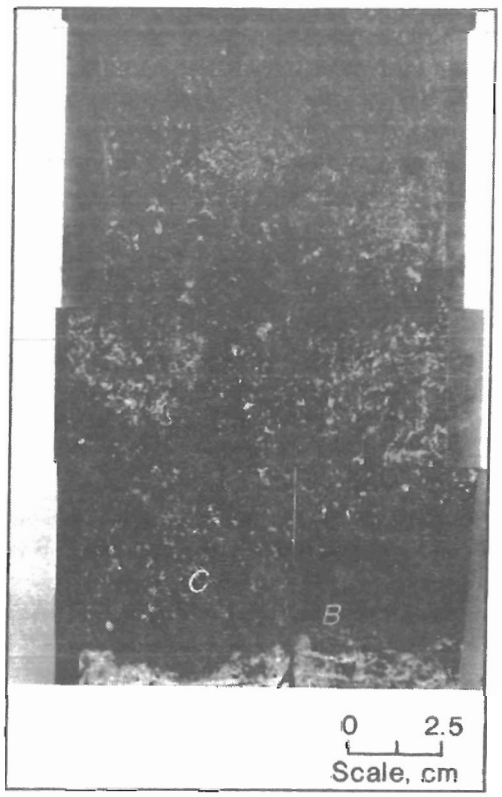

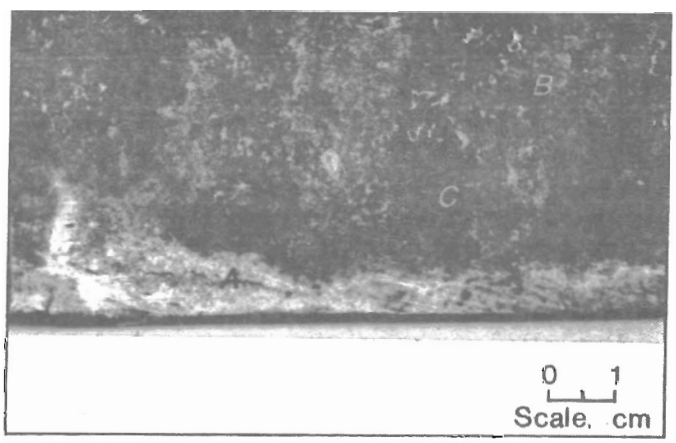

Cross-sectional views of leached massive 2 core. Leached interval of core (top). Injection end of leached core sample occurs at bottom. Close-up view of injection end (bottom). Both views show bleached horizontal layer (A), medium-gray channels of dissolution (B) finger upward from this leached layer into black, poorly to unleached material (C). White patches of calcite, some of which line vugs, can also be seen in black unleached matrix of rock.

Figure 7

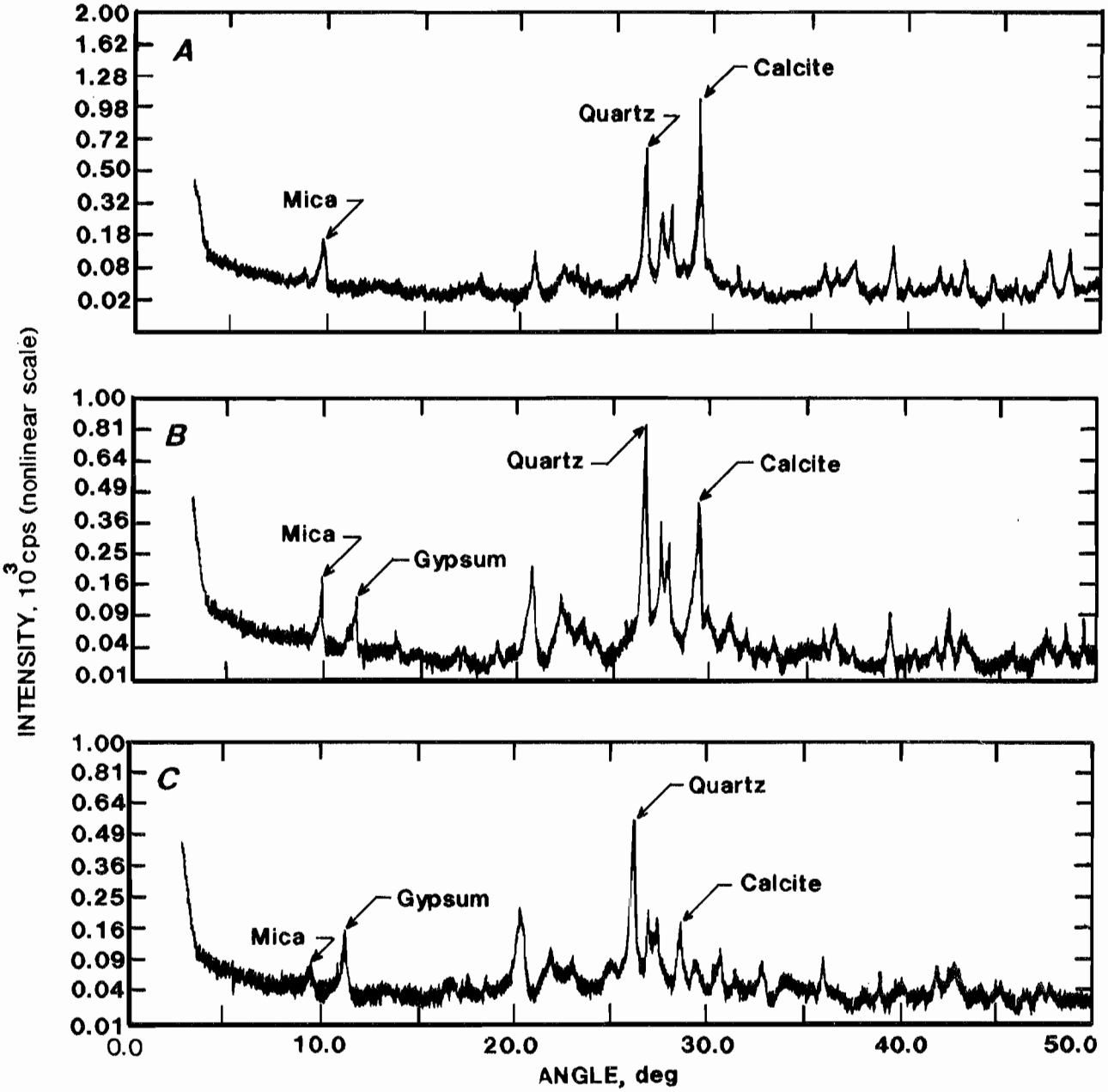

XRD patterns of samples from leached core. A, Unleached; B, partially leached; C, very leached.

interpreted that a majority of the Mn mineral(s) in the rock are poorly crystallized wad. The XRD pattern for the partially leached channels identified the same minerals as the least leached material. Differences are that the calcite peak was smaller and a new, fairly strong gypsum peak was present. The XRD pattern for the well-leached layer had an even smaller peak for calcite and a stronger gypsum peak than the other two patterns. Therefore, XRD results show that with leaching of massive 2 ore, some of the calcite is dissolved and gypsum is formed.

Modal Analysis

Polished-thin sections were made of the leached and unleached areas of the core. The texture of the rock was examined to determine how each mineral reacted with the

leach solution and to determine whether secondary precipitates were formed in the rock. By using transmitted light optical microscopy, it was easy to observe where black, opaque, Mn oxides had been dissolved and a clear to medium-orange-brown transparent residue was left behind (figure 8). Table 5 shows a comparison of modal analyses by point counting of unleached and leached polished-thin sections from the core leach experiment. The unleached Mn-mineralized arkosic sandstone is composed of approximately 70.6% matrix and 29.4% sedimentary grains. Of the total grains, 34.4% are quartz, 58.3% are feldspar, and 7.4% are mica. The leached mode of the rock consists of 29.6% matrix, 31.4% leached matrix, and 39.0% sedimentary grains. Of the total grains, 25.6% are quartz, 66.0% are feldspar, and 8.3% are mica. The leached mode cannot be extrapolated over the entire piece of core to arrive at the total amount of Mn oxide and calcite that was leached, as the selected thin sections represent only a small volume of the core sample. However, for the leached mode, the sum of the increase in void, clear leach residue, and Fe-stained leach residue compares favorably with the sum of the decrease in Mn minerals and calcite, 31.4% and 25.7%, respectively.

Figure 8

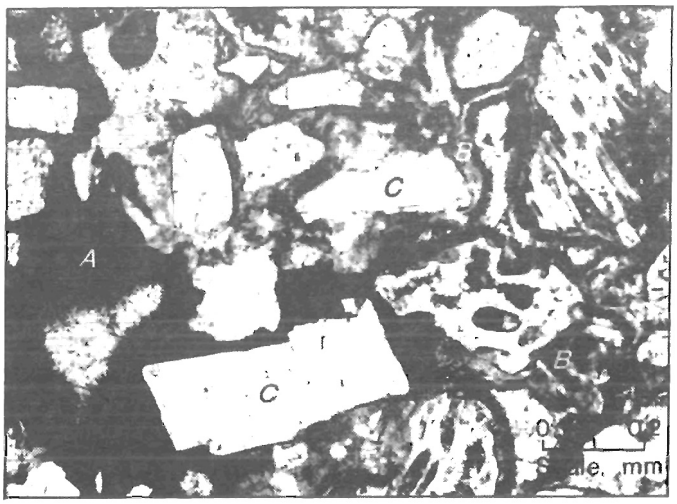

Photomicrograph of Si/Al-rich phase of leached residue after dissolution of Mn oxide minerals taken in transmitted light. Solid black is unleached wad (A), felsic grains are white (C), and mottled gray rims around felsic grains are leached residue (B).

Table 5.—Modal analyses of unleached and leached core tests for massive 2 sample

	Unleached		Leached	
	Average vol %	Standard deviation	Average vol %	Standard deviation
Minerals:				
Quartz	10.1	3.5	10.0	2.9
Plagioclase	2.1	1.4	2.2	1.5
Microcline	1.7	2.0	3.8	5.0
Feldspar with intergrowths	8.4	3.9	14.1	8.2
Altered feldspar	5.0	1.8	5.7	4.3
Muscovite	0.8	0.7	2.8	1.7
Biotite	1.3	0.8	0.4	0.3
Wad-cryptomelane	33.1	6.2	12.2	5.8
Si/Al rim	10.7	7.1	3.3	2.5
Calcite	18.5	3.2	14.1	6.0
Void	6.0	3.6	8.1	3.4
Leached residue	1.3	2.5	20.0	5.2
Leached Fe-stained rim	1.0	1.1	3.3	2.5
Total	100.0	NAp	100.0	NAp
Grains versus matrix:				
Grains	29.4	NAp	39.0	NAp
Matrix	62.3	NAp	29.6	NAp
Leached matrix	8.3	NAp	31.4	NAp
Total	100.0	NAp	100.0	NAp
Total grains:				
Quartz	34.3	NAp	25.6	NAp
Plagioclase	7.0	NAp	5.7	NAp
Microcline	5.7	NAp	9.8	NAp
Feldspar with intergrowths	28.5	NAp	36.0	NAp
Altered feldspar	17.1	NAp	14.6	NAp
Muscovite	2.9	Nap	7.3	NAp
Biotite	4.5	NAp	1.0	NAp
Total	100.0	NAp	100.0	NAp

NAp Not applicable.

Microprobe Analyses and Microimaging

Microprobe analyses and BSE imaging were performed on two of the polished-thin sections of the leached ore. One thin section included a leached channel in contact with unleached material and the other thin section included the beige horizontal band at the injection end of the core. Chemical microanalyses of individual minerals were performed on a JEOL 733 Superprobe equipped with WDS, an energy dispersive spectrometer (EDS), a BSE solid-state detector, and a secondary electron scintillation detector. For quantitative WDS analysis, the thallium acid phthalate (TAP) crystal was used for detecting Na, Al, and Si; the pentaerythritol (PET) crystal was used for S, K, Ca, and Ba; and the lithium fluoride (LIF) crystal was used for Fe and Mn. The Noran 5500 Task analysis program was used with the ZAF (Z stands for atomic number, A stands for adsorption, and F stands for fluorescence) correction program. Typical working parameters for characterization were a beam current of 10 nA and accelerating voltage of 15 kV. The detection limits for the elements are typically around 0.001 to 0.1 wt %. Low total weight percent oxides are due to contained water in the Mn oxides and perhaps the Si/Al phases. ZAF was also used for standardless semiquantitative EDS analysis.

Figures 9, 10, and 11 show BSE images of the microtexture of the rock after leaching. These images show what minerals were dissolved, what minerals were precipitated, and the spatial distribution of these minerals, which has a net effect on permeability of the leached rock. For example, one would expect voids to be left where Mn minerals or calcite cement had been completely dissolved. The BSE image shown in figure 9 shows a contact between leached and unleached wad and calcite. Some voids are present in the image and mostly represent shrinkage cracks. Some of the partially dissolved calcite, however, is rimmed with gypsum. Also, precipitates of manganese-barium sulfate [$(MnBa)SO_4$] and iron sulfate ($FeSO_4 \cdot 2H_2O$) occur in some of the areas where wad had rimmed felsic grains before it was dissolved.

Tables 6, 7, and 8 show representative WDS microprobe analyses of wad, cryptomelane, calcite, gypsum, and Si/Al-replaced feldspar (figure 5), as well as preleach (figure 5) and postleach Si/Al (figure 10). Cryptomelane contains Ba. The composition of Si/Al that has replaced part of a plagioclase grain can be compared with the thin-rim type of Si/Al. The composition of Si/Al that coats the interior of former pores (interstitial spaces) within the sandstone can be compared with similarly occurring Si/Al that was exposed to leach solution. The siliceous material replacing the plagioclase grain contains more Ca, K, and Na than the siliceous material rimming pores, and the rimming type of allophane that was exposed to leach solution is slightly more silica rich than the unleached example.

Figure 9

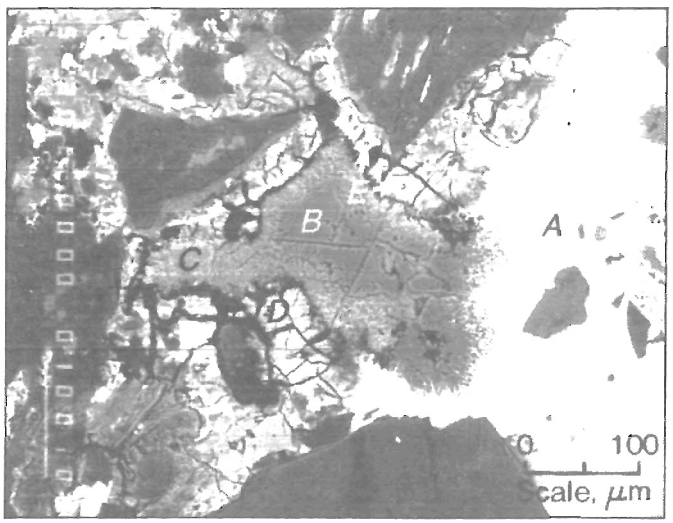

BSE image of contact between leached and unleached ore. Unleached Mn minerals (A) and calcite (B) are shown. In some of the areas where these two minerals were dissolved, gypsum (C), $(MnBa)SO_4$ (D), and $FeSO_4 \cdot 2H_2O$ (E) were precipitated. Otherwise, leached areas are black and filled with epoxy in this image.

Figure 10

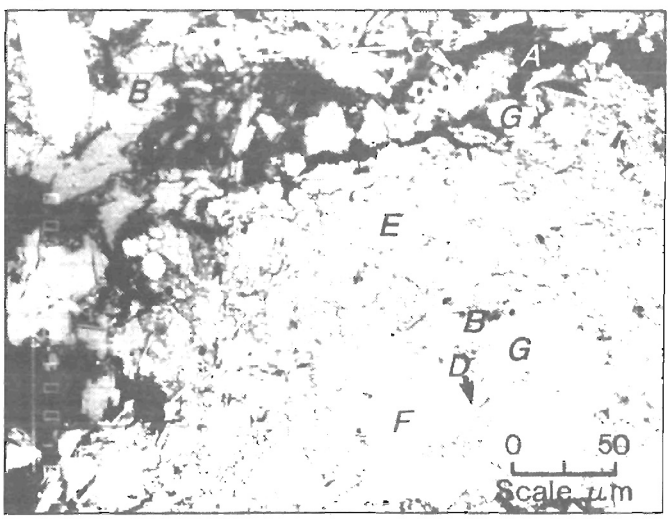

BSE image of leached texture after dissolving Mn minerals from oval-shaped interstitial area. Black void space (A) occurs around allophane-like Si/Al rim (B) that has lath-shaped crystals (C). Very small grains of mica (D), plagioclase (E), microcline (F), and quartz (G) are cemented by Si/Al material (B) and occur in Mn-leached ovoid.

Figure 11

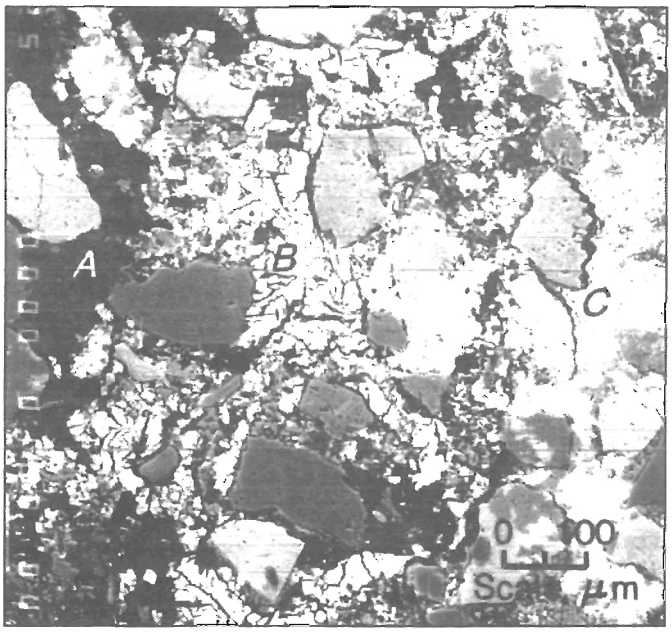

BSE image showing leached areas where Mn minerals were dissolved. Some of these areas are now filled with epoxy (A) and secondary precipitates of $MnSO_4$ (B) and gypsum (C).

Figure 10 is a BSE image of part of an oval-shaped interstitial area that has been well leached of Mn oxide. The thin rim of allophane-like Si/Al lines the ovoid. The abundant void space around the rim may indicate that it was partially dissolved or that this area contained only Mn minerals or calcite, which were totally dissolved. The lath shape of crystals of Si/Al suggests that the allophane-like material was not significantly dissolved. Dissolution of Mn minerals from the interior of the pore space unmasked very small grains of mica, plagioclase, microcline, and quartz, cemented by translucent Si/Al material. These very fine-grained sedimentary particles are not usually visible in the unleached rock.

The leached Si/Al material that was analyzed in table 8 are the two types of occurrences shown in figure 10, the rimming type and the cementing type. The cementing material is siliceous with a similar Si/Al ratio to the thin-rim type of Si/Al. Also, the translucent cementing material contains significant amounts of Fe, Mn, K, and S. It is believed that the allophane-like material in the rock is more visible after removal of Mn oxide and calcite from these leached areas. Lath-shaped crystals of the Si/Al phase also have been observed in the centers of some oval-shaped voids that have been leached of Mn oxide or calcite and are now filled with epoxy.

Table 6.—Representative WDS microprobe analyses of wad and cryptomelane

	Wad[1]		Cryptomelane[2]	
	Average wt %	Standard deviation	Average wt %	Standard deviation
Oxide:				
Al_2O_3	2.96	1.74	1.10	0.65
BaO	3.35	1.57	4.13	0.88
CaO	1.07	0.42	0.24	0.04
Fe_2O_3	2.97	0.52	2.05	0.36
K_2O	4.98	0.17	7.97	0.89
MnO_2	65.22	6.32	70.23	2.29
Na_2O	0.51	0.13	0.33	0.20
SiO_2	5.57	3.42	1.69	1.12
SO_4	1.44	0.49	0.85	0.67
Total	88.07	NAp	88.58	NAp
Stoichiometry:				
Al	0.46	0.27	0.18	0.10
Ba	0.18	0.08	0.23	0.05
Ca	0.15	0.06	0.04	0.01
Fe	0.30	0.05	0.22	0.04
K	0.85	0.02	1.43	0.15
Mn	6.04	0.67	6.81	0.22
Na	0.13	0.03	0.09	0.06
S	0.12	0.04	0.07	0.06
Si	0.74	0.44	0.23	0.15
Total	8.97	NAp	9.30	NAp
Mn+Fe+Al+Si	7.54	NAp	7.44	NAp
K+Ba+Na+Ca	1.31	NAp	1.79	NAp

NAp Not applicable.
[1]The number of analyses was 5; the cation basis is 16.
[2]The number of analyses was 6; the cation basis is 16.

Table 7.—Representative WDS microprobe analyses of calcite, gypsum, and Si/Al-replaced feldspar

	Calcite[1]		Gypsum[2]		Si/Al-replaced feldspar[3]
	Average wt %	Standard deviation	Average wt %	Standard deviation	Average wt %
Oxide:					
Al_2O_3	0.06	0.02	0.03	0.03	28.08
CaO	58.78	0.81	39.23	1.96	3.22
Fe_2O_3	0.00	0.00	0.07	0.07	0.06
K_2O	0.01	0.01	0.04	0.03	3.42
MnO_2	0.01	0.01	0.03	0.03	0.00
Na_2O	0.02	0.04	0.20	0.12	0.65
SiO_2	0.05	0.03	0.07	0.03	68.22
SO_4	0.02	0.04	54.87	13.61	0.06
Total	58.95	NAp	94.54	NAp	103.71
Stoichiometry:					
Al	0.00	0.00	0.00	0.00	2.75
Ba	0.00	0.00	0.00	0.00	0.00
Ca	1.00	0.00	0.97	0.16	0.29
Fe	0.00	0.00	0.00	0.00	0.00
K	0.00	0.00	0.00	0.00	0.36
Mn	0.00	0.00	0.00	0.00	0.00
Na	0.00	0.00	0.01	0.01	0.10
S	0.00	0.00	0.76	0.04	0.00
Si	0.00	0.00	0.00	0.00	5.67
Total	1.00	NAp	1.74	NAp	9.17
Si/Al	NAp	NAp	NAp	NAp	2.06

NAp Not applicable.
[1]The number of analyses was 4; the cation basis is 1.
[2]The number of analyses was 4; the cation basis is 4.
[3]The number of analyses was 1; the cation basis is 4.

Table 8.—Representative WDS microprobe analyses of preleach and postleach Si/Al

	Si/Al rim preleach[1]		Si/Al rim postleach[2]		Si/Al after leached Mn oxide[3]	
	Average wt %	Standard deviation	Average wt %	Standard deviation	Average wt %	Standard deviation
Oxide:						
Al_2O_3	21.30	3.64	24.64	0.76	17.85	3.27
BaO	0.03	0.01	0.04	0.03	0.12	0.09
CaO	3.12	1.64	2.48	0.21	0.37	0.41
Fe_2O_3	0.01	0.02	0.34	0.03	13.25	4.89
K_2O	3.04	0.35	3.05	0.16	7.74	1.67
MnO_2	0.83	0.28	0.78	0.06	8.93	7.61
Na_2O	0.34	0.17	0.65	0.11	0.64	0.57
SiO_2	51.87	8.28	64.61	2.01	48.11	7.71
SO_4	0.05	0.04	0.15	0.06	1.44	0.34
Total	80.59	NAp	96.74	NAp	98.45	NAp
Stoichiometry:						
Al	0.68	0.01	0.65	0.00	0.51	0.07
Ba	0.00	0.00	0.00	0.00	0.00	0.00
Ca	0.09	0.04	0.06	0.00	0.01	0.01
Fe	0.00	0.00	0.01	0.00	0.25	0.10
K	0.11	0.02	0.09	0.00	0.24	0.04
Mn	0.02	0.00	0.01	0.00	0.16	0.14
Na	0.02	0.01	0.03	0.00	0.03	0.03
S	0.00	0.00	0.00	0.00	0.00	0.00
Si	1.40	0.01	1.44	0.00	1.16	0.15
Total	2.32	NAp	2.29	NAp	2.36	NAp
Si/Al	2.06	NAp	2.22	NAp	2.27	NAp

NAp Not applicable.
[1]The number of analyses was 4; the cation basis is 4.
[2]The number of analyses was 2; the cation basis is 4.
[3]The number of analyses was 6; the cation basis is 4.

Figure 11 is a BSE image of the well-leached, white horizontal layer at the injection end of the core. The two light minerals that fill in between the felsic grains are manganese sulfate ($MnSO_4$) on the left (figure 11*B*) and gypsum on the right (figure 11*C*). The original texture of minerals rimming the felsic grains is destroyed where $MnSO_4$ has precipitated, but is still partially discernable where gypsum has precipitated. The source of the $MnSO_4$ precipitate is likely due to evaporation of saturated leach solution when the experiment had to be ended because of permeability loss. Tables 9 and 10 display representative EDS microprobe analyses of wad, $MnSO_4$, $(MnBa)SO_4$, barium sulfate ($BaSO_4$), calcite, gypsum, Ba-gypsum, and residual Si/Al after leaching.

Secondary Precipitation

By looking at the microtexture and mineral composition of the leached Artillery Peak ore, it is apparent that precipitation of Ca, Fe, and Ba sulfates is the cause for the progressive decrease in permeability during the core leach experiment.

Table 9.—Representative EDS microprobe analyses of wad, $MnSO_4$, $(MnBa)SO_4$, and $BaSO_4$, average weight percent

	Wad[1]	$MnSO_4$ and Fe[2]	$(MnBa)SO_4$[2]	$BaSO_4$[3]
Oxide:				
Al_2O_3	0.13	0.00	3.64	0.49
BaO	6.20	0.00	11.80	42.13
CaO	0.87	0.00	0.77	2.73
FeO	1.09	0.00	36.70	2.30
K_2O	2.77	0.07	0.70	1.06
MnO	[4]86.10	43.16	14.98	8.57
PbO	0.61	0.66	1.48	0.36
SiO_2	1.04	0.31	1.55	3.08
SO_4	1.19	55.80	28.38	39.28
Total	100.00	100.00	100.00	100.00
Chi-squared distribution	0.96	1.09	3.36	1.86
Stoichiometry:				
Al	0.03	0.00	0.07	0.01
Ba	0.56	0.00	0.08	0.30
Ca	0.21	0.00	0.01	0.05
Fe	0.21	0.00	0.55	0.03
K	0.81	0.00	0.20	0.02
Mn	13.55	0.51	0.22	0.13
Pb	0.04	0.00	0.00	0.00
S	0.17	0.49	0.31	0.45
Si	0.24	0.00	0.03	0.06
Total	15.82	1.00	1.47	1.05

[1]The number of analyses was 4; the cation basis is 16.
[2]The number of analyses was 3; the cation basis is 2.
[3]The number of analyses was 2; the cation basis is 2.
[4]MnO_2; most of the Mn in wad is in the Mn^{+4} state rather than the Mn^{+2} state.

Table 10.—Representative EDS microprobe analyses of calcite, gypsum, Ba-gypsum, and Si/Al, average weight percent

	Calcite[1]	Gypsum[2]	Ba-gypsum[3]	Si/Al[4]
Oxide:				
Al_2O_3	0.00	0.13	0.13	11.83
BaO	0.00	0.00	2.87	0.44
CaO	98.47	37.48	37.10	4.50
FeO	0.00	0.22	0.43	0.28
K_2O	0.00	0.06	0.15	3.04
MnO	0.43	0.24	0.67	2.55
PbO	0.00	0.50	0.00	0.00
SiO_2	0.00	0.66	1.75	72.32
SO_4	1.10	60.71	56.90	5.04
Total	100.00	100.00	100.00	100.00
Chi-squared distribution	1.17	1.07	0.91	1.00
Stoichiometry:				
Al	0.00	0.00	0.00	0.15
Ba	0.00	0.00	0.01	0.00
Ca	1.95	0.51	0.48	0.05
Fe	0.00	0.00	0.00	0.00
K	0.00	0.00	0.00	0.04
Mn	0.01	0.00	0.01	0.02
Pb	0.00	0.00	0.00	0.00
S	0.01	0.49	0.48	0.03
Si	0.00	0.01	0.02	0.78
Total	1.97	1.02	1.00	1.07
Si/Al	NAp	NAp	NAp	5.21

NAp Not applicable.
[1]The number of analyses was 1; the cation basis is 2.
[2]The number of analyses was 4; the cation basis is 2.
[3]The number of analyses was 2; the cation basis is 2.
[4]The number of analyses was 6; the cation basis is 2.

POSTLEACH GEOCHEMICAL CHARACTERIZATION

Leach Solution Chemistry

Table 4 lists typical concentrations of Mn, Fe, and Ca recovered in the leachate of the core leach test. When compared with the earliest solutions recovered from the GP-1 column leach experiment, where Ca leaching was most intense, the Mn concentration in the core leachate was lower than the column by about 35%, the Fe concentration in the core leachate was lower than the column leachate by about 95%, and the Ca concentration in the core leachate was higher than the column by about 23%. The leach solution was applied at 1 mL/min in the GP-1 column test and 0.005 mL/min in the core leach test. Although the flow rate of the core leach test was slower than the flow rate of the GP-1 column leach experiment, giving Mn more time to react, Mn recovery was lower in the core because of calcite dissolution. The GP-1 sample contained 1.3% calcite and the massive 2 sample contained 18.5% calcite. Acid-soluble calcite gangue dissolved during leaching in the core and resulted in high concentration of Ca in the leachate, as well as acid loss from the lixiviant. Calculations indicate that the solutions in the core were supersaturated with respect to gypsum shortly after the acid was injected into the core. This could have led to the observed loss of permeability in the core test as the precipitation of gypsum exceeded the porosity created by the dissolution of Mn. Figure 12 shows total recovered Mn, Fe, and Ca versus solution volume for the core leach test. Again, as in the GP-1 column leach test, Ca extraction initially exceeded Mn extraction.

Calcite Dissolution

Calcite dissolution also affected the efficiency of Mn leaching in the core by consuming acid, which resulted in lower Mn grades in the core test than in the column tests (table 4). The acidity of the leachate exiting the core was close to neutral with a pH of about 7. Because, as mentioned above, the efficient leaching of Mn oxide minerals requires that the pH of the leach solution be <2.5, calcite dissolution in the core test not only clogged pore channels by precipitation of gypsum, but also decreased the efficiency of the reductive dissolution of Mn oxides.

Figure 12

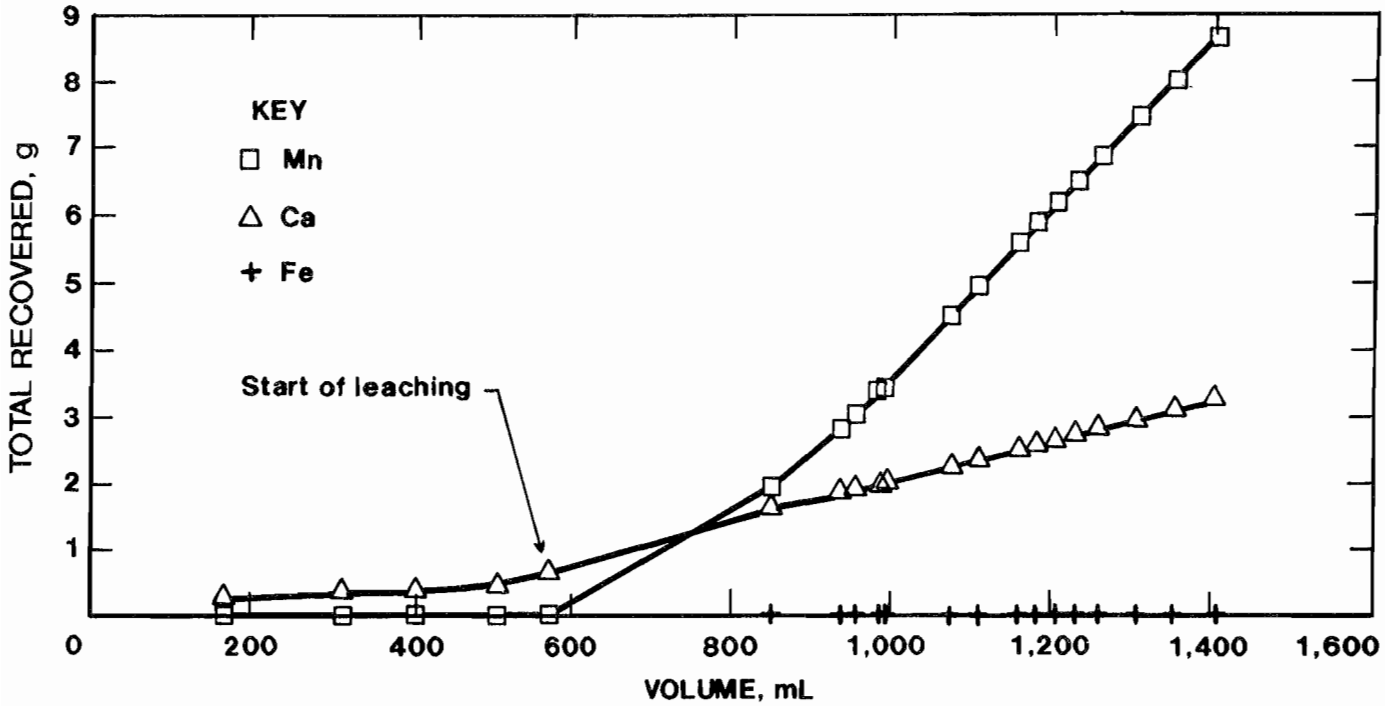

Total recovered versus solution volume for core leach test for massive 2 sample.

DISCUSSION

A comparison of column leach tests results with core leach test results demonstrate the complexity of the variables controlling the leaching process. Permeability changes that occurred in the core sample were so severe that continued leaching under those conditions was not possible. Although saturation with Ca sulfate minerals was observed in column testing of the ore, it did exhibit excellent recovery of the available Mn. However, under in situ conditions, saturation with Ca sulfate minerals arrested continued leaching of the Mn oxides in the core.

The success of evaluating any deposit for its potential as an in situ leach mining target depends on the leachability of the metal of interest, as well as the side reactions between the lixiviant and gangue minerals in the rock's matrix. This work has shown that calcite gangue mineral side reactions with a SO_2 lixiviant can have pronounced negative effects on the likelihood of successful in situ leaching at the Artillery Peak site.

ACKNOWLEDGMENTS

The authors would like to thank Norman Adamson, geologist, Twin Cities Research Center, and Bernhardt Saini-Eidukat, assistant professor, Department of Geosciences, North Dakota State University, Fargo, ND, for preleach and postleach mineralogy of the column leaching tests.

REFERENCES

Brink, S., B. Saini-Eidukat, D. Earley III, and R. Blake. Application of Petrographic Techniques To Assess In Situ Leach Mining Potential. USBM IC 9295, 1991, 14 pp.

Dietrich, R. V., J. T. Dutro, Jr., and R. M. Foose (eds.). A.G.I. Data Sheets for Geology in the Field, Laboratory, and Office. Am. Geol. Inst., 1982, sheet 58.2.

Khalafalla, S. E., and J. E. Pahlman. Selective Extraction of Metals From Pacific Sea Nodules With Dissolved Sulfur Dioxide. USBM RI 8518, 1981, 26 pp.

Kumke, C. A., C. K. Rose, F. D. Everett, and S. W. Hazen, Jr. Mining Investigations of Manganese Deposits in the Maggie Canyon Area, Artillery Mountains Region, Mohave County, Ariz. USBM RI 5292, 1957, 87 pp.

Marozas, D. C., S. E. Paulson, and L. M. Petrie. Evaluation of the Potential for Selective In Situ Leach Mining of Manganese Ores. Transactions, v. 292, 1992, pp. 1819-1828.

Pahlman, J. E., and S. E. Khalafalla. Leaching of Domestic Manganese Ores With Dissolved SO_2. USBM RI 9150, 1988, 15 pp.

Paulson, S. E., and H. L. Kuhlman. Laboratory Core-Leaching and Petrologic Studies To Evaluate Oxide Copper Ores of In Situ Mining. In Situ Leach Mining, USBM IC 9216, 1989, pp. 18-36.

Saini-Eidukat, B., D. Marozas, R. Blake, and N. Adamson. Implications of Rock Mineralogy and Texture on the Feasibility of In Situ Leach Mining of Mn-Bearing Iron Formations of Central Minnesota. Appl. Geochem., v. 8, 1993, pp. 37-49.

Sanford, R. S., and L. A. Stewart. Artillery Peak Manganese Deposits, Mohave County, Ariz. USBM RI 4275, 1948, 45 pp.

INT.BU.OF MINES,PGH.,PA 30110

★ U.S.G.P.O. 1995-609-012/20,017